Manhattan lattice Theta -point exponents from kinetic growth walks and exact results from the Nienhuis O(n) model

1994 J. Phys. A: Math. Gen. 27 1811

(http://iopscience.iop.org/0305-4470/27/6/009)

J. Phys. A: Math. Gen. 27 (1994) 1811–1826. Printed in the UK

Manhattan lattice Θ-point exponents from kinetic growth walks and exact results from the Nienhuis O(n) model

T Prellberg and A L Owczarek†
Department of Mathematics, The University of Melbourne, Parkville, Victoria 3052, Australia

Received 8 November 1993

Abstract. Kinetic growth walks (KGW) on the Manhattan lattice have previously been shown to be equivalent to the static problem of interacting self-avoiding walks on that lattice at the θ-temperature. Here, we illustrate how a complete set of exponents for the static problem, including the crossover exponent ϕ and surface exponents at the ordinary and special transition points, may be obtained from simulations of kinetic walks. In the process we find that $\phi \approx 0.430 \pm 0.006$ which encompasses the conjectured value $3/7 \approx 0.42857$ for the θ-point on an isotropic lattice. Our numerics confirm a predicted set of exponents for both the bulk and surface transitions in addition to results such as the exact internal energy at the bulk transition.

Furthermore, we point out that a recently examined variant of the Nienhuis O(n) model can be mapped onto θ-point walks on the Manhattan lattice which allows identification of the scaling dimensions for that problem and thereby provides a method for proving all the numerical conjectures.

1. Introduction

The collapse transition of a polymer in a dilute solution has been a focus of study in lattice statistical mechanics for several decades [1–3]. The basis for most lattice models is the self-avoiding walk which possesses the excluded volume interaction important in physical polymers. To mimic the complex monomer–solvent interactions that cause the collapse transition, an energy is associated with (non-consecutive) nearest-neighbour sites on the walk. The conformations of polymers (configurations of self-avoiding walks) have been argued to be described by the statistics of the magnetic O(n) model in the limit $n \to 0$ [4–6]. In recent years, progress has been made using the sophisticated techniques of conformal invariance [7] and the Coulomb gas [8] to predict the critical properties of polymer conformations [8, 9] in two dimensions. The collapse transition has similarly been argued to be described by a tricritical O(n) model in the limit $n \to 0$. Hence, there has been intense interest in lattice models that are related to O(n) models. One such model of loops on the honeycomb lattice with annealed vacancies, which we shall refer to as the Duplantier–Saleur (DS) model, has led to predictions for the relevant exponents at the θ-temperature [10]. This model has been the subject of many discussions [11–19] concerning its applicability to the θ-point. When considered as a walk model, it possesses a particular subset of next-nearest-neighbour interactions as well as the canonical nearest-neighbour monomer–mononer attraction. This has led to doubts over the relevance, in the renormalization group sense, of these unusual interactions. While it is generally accepted that the values of the radius of gyration exponent, ν, and the partition function exponent, γ, most likely take on

† e-mail: prel,aleks@mundoe.maths.mu.oz.au

0305-4470/94/061811+16$19.50

their DS values at the real two-dimensional θ-point, the crossover exponent and the surface exponents have been more controversial. Recently, it has been shown [18,20] that the surface exponents were not, initially, properly identified and new conjectures are closer to numerical results, although not in full agreement [19,21]. Numerical estimates [13,19,21–24] of the crossover exponent, ϕ, have consistently failed to be close to the exact conjecture of $3/7 \approx 0.428$ and have ranged from 0.48 to 0.90 [24,25]. It is usually acknowledged that this exponent is the most difficult to estimate [26].

The collapse transition in the DS model is related to the percolation of the vacancies and the temperature of the walk system maps to the percolation probability of the vacancies. This mapping is important in identifying the crossover exponent and at the θ-point the walks form the boundaries of the percolation clusters. An intimate relationship between θ-point walks and percolation had already been noticed [27] prior to the description of the DS model. This relationship involved models of dynamic polymerization as intermediaries. These models (KGW [28–30]) could be constructed to trap only by loop formation. This crucial property allows the identification of KGW on the honeycomb lattice [31] with the hulls of percolation clusters at threshold. The length of the walk is associated with the number of sites in the perimeter of the cluster. The percolation probability of the cluster controls the relative probability of turning left rather than right in the KGW. These smart KGW were also found to map to the static problem of interacting self-avoiding walks on that lattice with a particular subset of next-nearest-neighbour interactions [27]. This connection between some static-walk problem and the percolation transition inspired Duplantier and Saleur to write down their model [10] where, as mentioned above, the percolation probability was now associated with the walk-model temperature. In a parallel development, Ziff examined the critical properties of percolation hulls [32] and confirmed a set of exponents for this problem. Saleur and Duplantier [33] obtained the exact fractal dimension of the hulls (related to $1/\nu$ for walks) of percolation clusters by using Coulomb gas methods.

The mapping between the KGW and θ-walks allows the identification of the size exponent, ν, and the partition function exponent, γ. Studies of KGW have previously focused on these exponents. In this paper we shall show how to extract the thermal-crossover exponent and surface exponents for static-collapse problems from KGW. In particular, we shall concentrate on the case of the Manhattan lattice. The case of smart KGW on the honeycomb lattice is currently being examined [34]. We do this because KGW on the Manhattan lattice are by their nature 'smart' without the need for additional constraints. Therefore, they map onto a static problem with only *nearest-neighbour* interactions. Secondly, we shall show that the static problem can be mapped precisely onto an exactly solvable vertex model from which all the exponents can be confirmed. These two approaches allow us to give a set of exact values for the standard exponents (see tables 1 and 2).

Table 1. Best estimates and exact conjectures for the bulk exponents for θ-point Manhattan walks from KGW simulations. These are to be compared to the values for the Duplantier and Saleur model.

Exponent	ν	γ_t	α_t	ϕ
Estimates	0.571(2)	0.8575(15)	0.8575(15)	0.430(6)
Exact	4/7	6/7	6/7	3/7
DS walks	4/7	8/7	6/7	3/7

Table 2. Best estimates and exact conjectures for the surface exponents. The exponent γ_{11} is obtained via the Barber scaling relation.

Exponent	γ_1^{ord}	γ_{11}^{ord}	γ_1^{sp}	γ_{11}^{sp}	ϕ_s
Estimates	0.429(2)	−0.571(2)	1	4/7	0.382(3)
Exact	3/7	−4/7	1	4/7	8/21
DS walks	4/7	−4/7	8/7	4/7	8/21

Much is already known about KGW on the Manhattan lattice. Bradley [35, 36] has previously mapped this model onto the static walk problem with the partition function

$$Z_N(\omega) = \sum_{\varphi_N} \omega^{M(\varphi_N)} \tag{1}$$

where the sum is over all configurations φ_N of length N. The configurations are all self-avoiding loops allowed on the Manhattan lattice and have $M(\varphi_N)$ nearest-neighbour contacts. This mapping holds at an inverse temperature of $\beta = (\log 2)/2$, where $\omega = e^{\beta}$ is the Boltzmann weight associated with each nearest-neighbour contact. By also mapping to the problem of bond percolation, Bradley was able to identify that $\nu = 4/7$ and $\gamma = 6/7$. This applies to the related models of Gunn *et al* [37], Roux *et al* [38] and series work is in accord with these results [39]. One assumption in Bradley's work is that KGW on the Manhattan lattice (MKGW) close with probability 1. This has recently been rigorously proved [40]. The MKGW are also related to the Ruijgrok–Cohen Lorentz lattice gas [41, 42], where extensive simulation has also confirmed Bradley's exact results for ν and γ with a very high degree of precision.

The collapse transition in the interacting self-avoiding walk problem is brought about by preferentially weighting nearest-neighbour contacts. We have stochastically enumerated KGW on the Manhattan lattice, up to lengths of 10^6, keeping track of the average number of such contacts and their fluctuations. This allows the calculation of the internal energy and specific heat of the KGW over a range of lengths. This gives us the ability to find estimates of specific-heat exponent, α, and crossover exponent, ϕ, (see [26] for instance) which are related to each other via a scaling relation. We have also enumerated KGW stochastically on a particular half-plane formation with absorbing and reflecting boundary conditions, which we argue can be mapped to the static problem at the ordinary and special transition points, respectively. From these simulations we find values for the partition function exponents γ_1^{ord} and γ_{11}^{ord} and the surface-crossover exponent ϕ_s. The special point exponents, γ_1^{sp} and γ_{11}^{sp}, are clear from the existence of the mapping and the Barber scaling relation. In fact, these surface exponents can all be derived from other arguments [43]. From this set of estimates exact conjectures can be made which in turn lead to a set of scaling dimensions (table 3).

Table 3. Relevant scaling dimensions for θ-point Manhattan walks.

Exponent	x_h	x_t	x_{tt}	x_h^{ord}	x_t^{ord}	x_h^{sp}	x_t^{sp}
Manhattan value	1/4	1/4	5/4	1	2	0	1/3
DS walks	0	1/4	5/4	1	2	0	1/3

A particular O(n) model suggested by Nienhuis [44, 45] on the square lattice has recently been examined [46] and Bradley's values for the exponents ν and γ found. This, we shall

show, is no coincidence. In fact, we show that Manhattan walks at $\beta = (\log 2)/2$ can be mapped precisely onto this loop model via the model of interacting trails on the L-lattice. The bulk scaling dimensions found there are in agreement with those in table 3. The surface scaling dimensions can be found in the O(n) model from a finite-size calculation, similar to that in [47].

We are now in a position to compare the scaling dimensions for the θ-point walks on the Manhattan lattice to those of the DS model. In terms of conformal field theory, both are non-reflection positive (non-unitary) theories with a central charge $c = 0$. In fact, the only difference between this set of scaling dimensions and those for the DS model is that in the DS model $x_h = 0$. It seems that Manhattan walks pick up the 'even' bulk scaling dimensions, as in percolation [9] (Batchelor's full set of bulk-scaling dimensions are precisely those of percolation). The relevant surface-scaling dimensions are identical.

The paper is divided as follows. The definition of the model, the method of simulation and the techniques of analysis of the results are presented in section 2. The bulk and surface are treated separately inside this section. Furthermore, the special and ordinary point simulations are separated. The mapping to the O(n) model is explained and discussed further in section 3. Finally, a short set of conclusions is given in section 4.

2. Simulations

2.1. The model

Before we describe the simulations, we will define the model in more detail. We consider kinetically grown self-avoiding walks on the Manhattan lattice. The Manhattan lattice is a directed square lattice with a network of alternating 'one-way streets', i.e. neighbouring parallel bonds have opposite direction.

A KGW on this lattice is a walk where every step is chosen from the available ones with equal probability p. For the Manhattan lattice, the possible number of steps is at most two, as each site has two exiting bonds, each of which is chosen with probability $p = 1/2$. However, if one of the bonds is prohibited (which corresponds to a nearest-neighbour interaction) the next step is naturally taken with probability 1. Moreover, due to the geometry of the lattice, this step will create a further nearest-neighbour interaction, so that in the corresponding interacting model $\omega^2 = 2$, where $\omega = \exp(\beta)$ is the Boltzmann weight of a single nearest-neighbour interaction [36].

If we let the walk start at a ghost site in the middle of a bond, and terminate the walk when it re-enters the same bond, then the probability p_φ of a loop φ produced in this process is in direct relation to the Boltzmann weight of the same loop in a model with nearest-neighbour interactions of Boltzmann weight $\omega = \sqrt{2}$, as we can write

$$p_\varphi = 2^{-N} 2^{M/2} \tag{2}$$

where N is the length of the loop and M denotes the number of nearest-neighbour interactions. Therefore, if we form the sum P_N over all kinetically grown loops φ_N of length N with their respective probabilities p_{φ_N}

$$P_N = \sum_{\varphi_N} p_{\varphi_N} \tag{3}$$

and define the partition function of the interacting loop model as

$$Z_N^{(I)}(\omega) = \sum_{\varphi_N} \omega^{M(\varphi_N)} \tag{4}$$

we get equivalence at $\omega^2 = 2$ in the form

$$P_N = 2^{-N} Z_N^{(t)}(\sqrt{2}). \tag{5}$$

Furthermore, the loop formation rate P_N is clearly related to the the probability Q_N of an open walk of length N by

$$P_N = Q_N - Q_{N+1} \tag{6}$$

which in turn is related to the partition function $Z_N^{(w)}$ for interacting walks at $\omega^2 = 2$. Using our construction starting at a ghost site, we have a weight p_φ of walks which can be bounded by the corresponding Boltzmann weight in an interacting model from both sides, as p_φ does not contain the information about interactions with the last site, because these only matter for the next step. On the other hand, as explained above, the occurrence of a blocked bond already accounts for a nearest-neighbour interaction at the next site. Therefore, p_φ overcounts the number M of interactions by at most one and undercounts it by at most two, so that

$$Z_N^{(w)}(\sqrt{2}) \sim 2^{-N} Q_N. \tag{7}$$

This, together with equation (6) and the proven fact [40] that walks close with probability one, can be used to show that that the entropic exponents γ_t and α_t are equal,

$$\gamma_t = \alpha_t \tag{8}$$

provided the probability of an open walk decays with a power law. Then, we can identify

$$P_N \sim p_0 N^{\alpha_t - 2} \qquad \text{and} \qquad Q_N \sim p_0 N^{\gamma_t - 1} \tag{9}$$

which by equation (6) implies the equality in (8).

2.2. *Method*

We have generated walk configurations up to a length of 10^6 steps. The occupied sites of the walk are stored in a hash table [48], with the hash index being computed from the coordinates in order to facilitate direct access to lattice sites via the lattice coordinates without having to store the whole lattice. The size of the hash table needs to exceed the maximal walk length only slightly, so that generation of a walk of length N (provided it does not trap) requires time $O(N)$ and memory $O(N)$. When a walk reaches the desired maximal length or gets trapped, a new one gets generated. This ensures the statistical independence of the walks sampled at fixed length.

For the generation of random numbers we used the routine `ranf()` from the random number generator package `ranlib.c` which utilizes base code from [49]. This code is the implementation of a mixed-linear congruential-generator algorithm [50]. This package has proved to be comparatively reliable [51], an important consideration in view of recent doubts about the quality of these generators within Monte Carlo simulations [52, 53]. In order to try to incorporate the statistical errors from the random number generator into our error estimation we produced independent runs of various lengths using different seeds.

While the walks were generated, we sampled data at equidistantly spaced lengths, keeping track of the desired quantities including their fluctuations. Although the generated walks are independent of each other, this introduces highly correlated data (between different lengths), as every walk of a given length has contributed to all data sets of shorter length. We notice that this can be effectively overcome by calculating quantities using an exponential spacing, as we shall see below.

2.3. *Bulk simulations*

Here, we have generated three independent runs of 10^7 samples of length 10^4, 10^6 samples of length 10^5 and 3.15×10^5 samples of length 10^6. As an example, the generation of the 3.15×10^5 samples of the longest walks ($N = 10^6$) was completed on an IBM RISC 6000/530 in about 85 CPU days.

From the simulations on an unbounded Manhattan lattice we were able to compute estimations for the length-scale exponent ν_t and the entropic exponents γ_t and α_t. We estimate finite-size approximations $\nu_{t,N}$ from the mean-square end-to-end distance $\langle R^2 \rangle_N$ which is assumed to scale as

$$\langle R^2 \rangle_N \sim r_0 N^{2\nu_t} \tag{10}$$

by forming

$$2\nu_{t,N} = \log_2 \frac{\langle R^2 \rangle_N}{\langle R^2 \rangle_{N/2}}. \tag{11}$$

A graphical extrapolation versus $1/N$ towards infinity gives $\nu_t = 0.571(2)$. Here, as well as in all the other exponent estimations, there is clear evidence of the data correlation. However, as we have chosen exponential spacing of the data points for the finite-size estimators, the error due to the correlations seems to be smaller than the fluctuations due to statistical error in the single data points, and can therefore be neglected. We also point out that this extrapolated value differs little from the estimates of the last decade of the lengths sampled and hence, the final result will essentially be the same as if we had chosen $\sqrt{1/N}$ instead of $1/N$.

For the entropic exponents $\alpha_t = \gamma_t$ we use the finite-size approximations

$$1 - \gamma_{t,N} = \log_2 \frac{Q_N}{Q_{N/2}} \tag{12}$$

and extrapolate towards infinity to get $\gamma_t = 0.8575(15)$.

The calculation of the internal energy, given by

$$U_N = \frac{\langle M \rangle}{N} \tag{13}$$

where M is the number of nearest-neighbour interactions and specific heat, given as

$$C_N = \frac{\langle M^2 \rangle}{N} - \frac{\langle M \rangle^2}{N} \tag{14}$$

of the KGW give us the ability to find estimates of the specific heat exponent, α and the crossover exponent, ϕ, [26] which are related to each other via the scaling relation

$$2 - \alpha = 1/\phi. \tag{15}$$

At the tricritical-like point in static-collapse problems [26] the internal energy U_N of walks of length N behaves asymptotically as

$$U_N \sim U_\infty + u_0 N^{(\alpha-1)\phi} \tag{16}$$

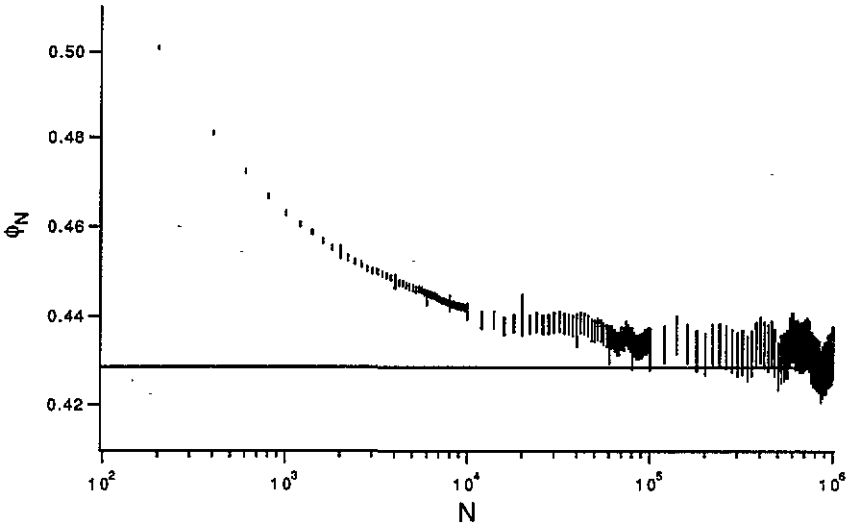

Figure 1. Local estimates ϕ_N of the crossover exponent ϕ are plotted against the length N from the internal energy data assuming $U_\infty = 2/3$. The horizontal line corresponds to the exact value $\phi = 3/7$.

while, if $\alpha < 0$, the specific heat C_N behaves as

$$C_N \sim C_\infty + c_0 N^{\alpha\phi}. \tag{17}$$

By calculating both the internal energy and specific heat we can either obtain two estimates of ϕ using the scaling relation (15) or alternatively use the relation to check the accuracy of our results.

Moreover, as we know the limiting value of the internal energy exactly, $U_\infty = 2/3$ (see section 3), we can use this knowledge to get a very accurate estimate for ϕ using the finite-size estimations

$$\phi_N - 1 = \log_2 \frac{2/3 - U_N}{2/3 - U_{N/2}} \tag{18}$$

with errors computed from the respective fluctuations.

We point out here that the convergence of the specific heat is equivalent to a *decrease* of the fluctuations of the internal energy as the walks grow longer,

$$\sigma^2(U_N) \sim \frac{C_N}{N} \tag{19}$$

so that the error in the estimation of U_N is inversely proportional to the product of sample size and walk length, i.e. it is inversely proportional to the run time T *independently* of the lengths of the created walks. Therefore, it is advantageous to create as large walks as possible in order to get beyond finite-size corrections-to-scaling and see the true asymptotic behaviour without the need for further extrapolation.

The finite-size estimations for ϕ are shown in figure 1. Clearly, there are strong finite-size corrections present, and the asymptotic value of $\phi = 0.430(6)$ is reached well beyond lengths of 10^3. In fact, if one tries to extrapolate from data for lengths up to 10^2, the value one obtains for ϕ is well above 0.5, in correspondence with estimations of ϕ from walks of lengths less than $N = 300$ [23]. The estimates of ϕ from the specific heat data are consistent with the internal energy data.

We do not use any further extrapolation methods, as we have simulated walks of such considerable length and cannot reasonably estimate with any precision the corrections-to-scaling. On the other hand, examination of figure 1 suggests that the estimates of ϕ, for example, from the longest walks, are close to their asymptotic value, while estimates from shorter walks clearly show a downward drift. The results of our estimation for all the bulk exponents are in table 1. Each result encompasses the predicted exact value. Assuming $\phi = 3/7$, we further get a consistency check by estimating $U_\infty = 0.66667(1)$. The application of this extrapolation method to the specific heat data is shown in figure 2, with both the actual data and the extrapolated values plotted. We estimate $C_\infty = 3.56(4)$.

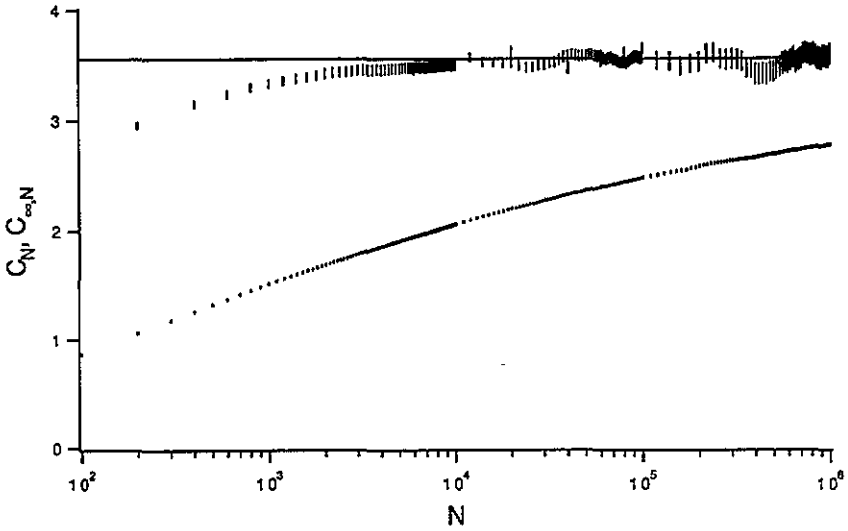

Figure 2. Local estimates $C_{\infty,N}$ of the thermodynamic limit specific heat C_∞ are plotted against the length N. Also, the values of the raw specific heat C_N are plotted for comparison. The horizontal line corresponds to the value 32/9.

2.4. Surface simulations

For the surface simulations we restrict the walk to grow on a half plane. The boundary is chosen such that the walk cannot return to its origin, as seen in figure 3. We are interested in simulating the kinetic problem equivalent to the static model with partition function

$$Z_N^{(1)}(\omega, \omega_s) = \sum_{\varphi_N} \omega^{M(\varphi_N)} \omega_s^{M_s(\varphi_N)} \tag{20}$$

where $\omega = \sqrt{2}$, for various values of ω_s. This is the partition function for walks that have one end attached to the surface in the half plane with a surface (inverse) temperature of $\log \omega_s$. The number of surface contacts of the half-plane configuration φ_N is $M_s(\varphi_N)$.

We can simulate KGW corresponding to a range of surface interactions as follows. First, a walk begins at a special surface site and may walk only in a half plane as shown in figure 3. When a walk takes a step that leaves the surface into the other half of the lattice it is terminated and a new walk starts. By changing the probability of the walk taking this step

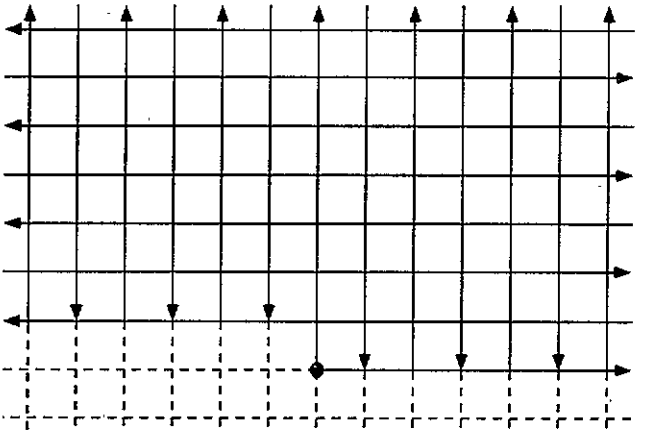

Figure 3. The boundary shape of the lattice used in the surface simulations. The broken part of the lattice indicates that part of the lattice unused by the walk. A walk can move along the surface freely and at every second site can choose with probability $1 - p_s$ to cross the boundary and enter the broken section of the lattice. In this case the walk is terminated and a new configuration begun. For the ordinary point absorbing boundary conditions, with $p_s = 1/2$, are used while for the special point reflecting boundary conditions, with $p_s = 1$, are utilized. Every walk begins at the site marked with a bullet.

we change the weight of the corresponding configuration. As the sites adjacent to a surface bond can only be entered once, the probability p_s of the walk not entering the surface is directly related to the surface interaction ω_s. If the walk does not enter the surface, the next step will be along the surface, so that we have

$$\omega_s^2 = 2p_s. \tag{21}$$

Therefore, we are able to cover the full range from infinite repulsion $\omega_s = 0$ to a maximal finite attraction $0 \leqslant \omega_s \leqslant \sqrt{2}$. The probability $Q_{s,N}$ of continuing configurations at particular length N is related to the partition function $Z_N^{(1)}(\omega, \omega_s)$ for walks with one end attached to the surface, via

$$Q_{s,N} \sim 2^{-N} Z_N^{(1)}(\sqrt{2}, \sqrt{2p_s}) \tag{22}$$

similar to (7). Hence, estimates of the partition function exponent γ_1 can be found via a formula analogous to (12) as

$$1 - \gamma_{1,N} = \log_2 \frac{Q_{s,N}}{Q_{s,N/2}}. \tag{23}$$

The exponent γ_{11} related to the partition function of walks with both ends attached to the surface can be found via the probability of closure

$$P_{s,N} = Q_{s,N} - Q_{s,N+1} \tag{24}$$

provided $Q_{s,N}$ decays to zero as a power law (which holds at the ordinary point though not at the special point), as

$$1 - \gamma_{11,N} = \log_2 \frac{P_{s,N}}{P_{s,N/2}} \tag{25}$$

or the Barber scaling relation

$$\nu + \gamma = 2\gamma_1 - \gamma_{11}. \tag{26}$$

2.4.1. The ordinary point. Here, we choose the kinetic growth probability $p_s = 1/2$, which corresponds to $\omega_s = 1$, i.e. no interaction. As the surface increases the trapping probability, the generation of long walks is very inefficient. Therefore, we generated a sample of 10^6 walks of lengths up to only 2×10^4. To achieve this number of completed walks of that length (2×10^4) we had to generate a total of 157 226 874 samples.

Using finite-size estimators of the exponential decay of the trapping rate (see figure 4), we estimate $\gamma_1^{\text{ord}} = 0.429(2)$, which covers the exact value $\gamma_1^{\text{ord}} = 3/7$. Furthermore, using the Barber scaling relation (26), this leads to an estimate of $\gamma_{11}^{\text{ord}} = -0.571(2)$, which can be compared to the exact value $\gamma_{11}^{\text{ord}} = -4/7$.

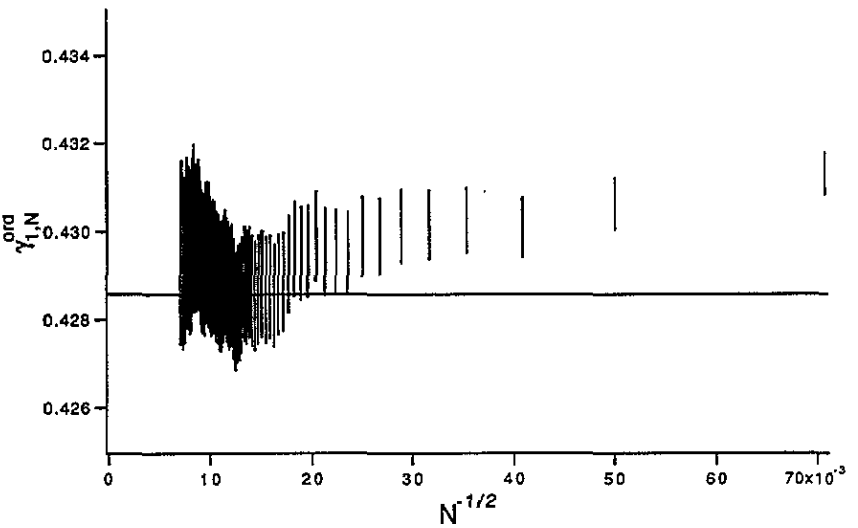

Figure 4. Local estimates $\gamma_{1,N}^{\text{ord}}$ of the closure exponent γ_1^{ord} are plotted against $N^{-1/2}$. The horizontal line corresponds to the value $\gamma_1^{\text{ord}} = 3/7$.

2.4.2. The special point. Here, we choose the kinetic growth probability $p_s = 1$, i.e. the surface reflects the walk completely, which corresponds to $\omega_s = \sqrt{2}$ and generate a sample of 10^6 walks of lengths up to 2×10^5. In contrast to the ordinary point simulations, every attempted generation resulted in a walk of the maximum length, because there is no possibility of closure, and hence the lengths possible were much greater. The generation of the 10^6 samples of length 2×10^5 took approximately 24 days CPU time on an IBM RISC 6000/560.

As the walk is completely reflected and there is no loop formation by construction, this leads immediately to a value of $\gamma_1 = 1$, which is clearly different from $\gamma_1^{\text{ord}} = 3/7$. Therefore, $\omega_s = \sqrt{2}$ is a candidate for the special point. In our simulations we now keep track of the number of surface contacts M_s, which is supposed to scale as

$$M_{s,N} \sim m_0 N^{\phi_s} \tag{27}$$

with a surface crossover exponent ϕ_s strictly between the values 0 (ordinary regime, walk not bound to the surface) and 1 (walk bound to the surface). We extract ϕ_s using finite-size estimations (see figure 5), obtaining a value of $\phi_s = 0.382(3)$, which clearly indicates

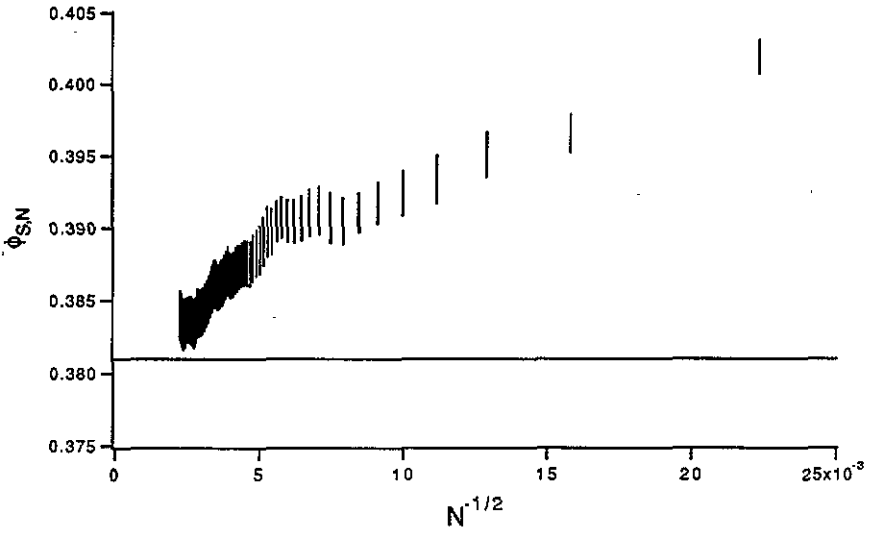

Figure 5. Local estimates $\phi_{s,N}$ of the surface crossover exponent ϕ_s are plotted against $N^{-1/2}$. The horizontal line corresponds to the exact value $\phi_s = 8/21$.

that we are at the special point and hence the absorption transition (inverse) temperature is $\beta_s = (\log 2)/2$. Moreover, it covers the exact value $\phi_s = 8/21 \approx 0.38095$ for DS walks.

We therefore conclude that $\gamma_1^{sp} = 1$ and, by using the Barber scaling relation, that $\gamma_{11}^{sp} = 4/7$. One point worth mentioning is that here we again have very strong finite-size corrections-to-scaling which necessitate the use of very long walks. Data from shorter walks clearly lead to a value of ϕ_s which is larger, which is reminiscent of other work using walks of lengths less than $N = 300$ [21].

3. Nienhuis O(n) loop model

The model suggested by Nienhuis [44, 45] and recently discussed by Batchelor [46], which we now show is equivalent to interacting walks on the Manhattan lattice at the θ-temperature, is a nine-vertex loop model on the square lattice derived from the O(n) model. The nine allowed vertices are given in figure 6. The loop model is obtained from the n-vector spin model [54] via a high-temperature expansion [55]. Only certain manifolds have been amenable to exact techniques and the point of most interest is known as the branch 0. The Boltzmann weights ρ_j ($j = 1, \ldots, 9$) are parametrized by two variables, v and w, as

$$\rho_1, \ldots, \rho_9 = (v + w, v, v, w, w, 0, 0, v, w) \tag{28}$$

and branch 0 is the point $v = w = 1/2$. Because two Boltzmann weights are zero this manifold is more properly referred to as a seven-vertex model. The partition function is given [46] as

$$Z = \sum_G \rho_1^{m_1} \ldots \rho_9^{m_9} n^L \tag{29}$$

where m_j is the number of vertices of type j and L is the number of loops of fugacity n. This is a member of the exactly solvable set of dilute loop models. The equivalent

O(n) spin model has the ρ_j as the prefactors of different spin–spin interactions, with the number of spin components being n. This model is equivalent to a q-state Potts model with $q = (n+1)^2$ via a Temperley–Lieb equivalence [56] and hence to a six-vertex model with crossing parameter λ given as $n = 2\cos\lambda - 1$. The case of interest here is the limit of a single loop given by vanishing loop fugacity, $n \to 0$. We note immediately that this means the case of interest is equivalent to the $q = 1$ Potts model ($\lambda = \pi/3$) which is well known [57] to be related to percolation. The model is also equivalent [44, 46] to a manifold of the three-state nineteen-vertex model with four weights equal to zero and hence is denoted a fifteen-vertex model. As usual there is a related (spin-1) quantum spin chain [46] also.

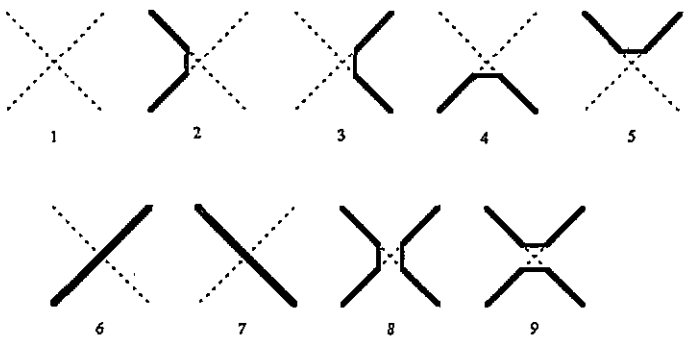

Figure 6. The nine configurations of the O(n) model on the square lattice with the heavy bold lines representing sections of the loop.

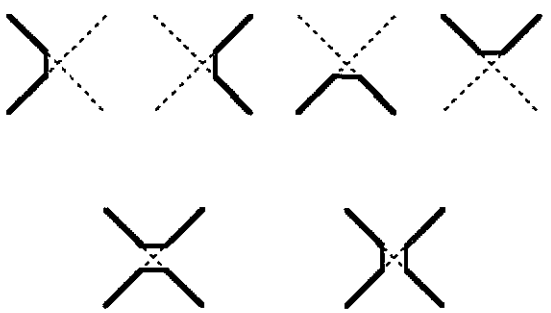

Figure 7. The six-vertex configurations of trails on the L-lattice with the heavy bold lines representing steps of the trail.

To begin let us consider only $v = w = 1/2$, branch 0 and later briefly mention the case $v + w = 1$ (which is not a restriction on the model above). In the limit $n = 0$ one is essentially considering a single loop with the six vertices, as in figure 7, and each vertex has equal weight. Immediately one can see that these configurations are trails on the L-lattice with each step given a fugacity 1/2 and each contact given a weight 2 in order that each vertex has equal weight. More explicitly, the loop model partition function can be expanded as

$$Z = 1 + n \sum_{G_1} \left(\tfrac{1}{2}\right)^{m_2+m_3+m_4+m_5+m_6+m_8+m_9} + O(n^2) \tag{30}$$

where G_1 is the set of configurations of a single loop. Let $m = m_8 + m_9$ be the number of contacts in a configuration. The total length of the walk N is given by

$$N = m_2 + m_3 + m_4 + m_5 + 2m \tag{31}$$

which means that

$$\begin{aligned}(\mathcal{Z} - 1)/n &= \sum_{G_1} (\tfrac{1}{2})^{N-m} + \mathcal{O}(n) \\ &= \sum_{N} (\tfrac{1}{2})^{N} \sum_{m} c_N(m) 2^m + \mathcal{O}(n)\end{aligned} \tag{32}$$

where $c_N(m)$ is the number of trails on the L-lattice with m contacts. The first term in this expansion (32) is then the generating function for trails on the L-lattice with each contact given a weight 2 at the critical monomer fugacity. The configurations involved are then simply interacting trails on this lattice at an inverse temperature $\beta_{\text{trails}} = \log 2$. Correlation functions of the O(n) model then pick up this set of configurations and Boltzmann weights when $n = 0$. Interacting trails on the L-lattice can be mapped, via a bond-to-site mapping (the Manhattan lattice is the *covering* lattice of the L-lattice), to interacting walks on the Manhattan lattice [36]. The interacting-walk problem is at an inverse temperature of $\beta = (\log 2)/2$ since each contact of the trails leads to two nearest-neighbour contacts in the walk model. The free energy for this model is $-\beta f = \log 2$ as given by Bradley for θ-walks and Batchelor for the equivalent six-vertex model at $\lambda = \pi/3$.

One result that can be immediately deduced is that the internal energy of IMSAW at the θ-point is $U_\infty = 2/3$. This comes from the fact that the internal energy of IMSAW is twice the average value of m/N (the number of trail contacts) and this average is 1/3 by symmetry (there is a mapping of the loop model onto a two-colour dense loop model [46, 58]).

Batchelor [46] has identified the bulk scaling dimensions X_j of this O(n) model as

$$X_j = 2\Delta(0, j) = (j^2h^2 - 1)/2h(h + 1) \tag{33}$$

where Δ is given by the Kac formula (for instance see [37])

$$\Delta(p, q) = \frac{[p(h + 1) - qh]^2 - 1}{4h(h + 1)} \tag{34}$$

with h related to the central charge as

$$c = 1 - \frac{6}{h(h + 1)} \tag{35}$$

and

$$h + 1 = \pi/\lambda. \tag{36}$$

Hence, for $n = 0$ we have $h = 2$ and $c = 0$ with

$$X_j = \frac{4j^2 - 1}{12}. \tag{37}$$

Now, this is precisely the set of scaling dimensions for percolation [9] and the 'even' subset of the scaling dimension (that is, x_L with L even) identified [9] for the DS model as

$$x_L = (L^2 - 1)/12. \tag{38}$$

Now, if a scaling dimension satisfies $x \leqslant 2$ it is associated with a relevant scaling field and hence the relevant scaling dimensions associated with IMSAW are exactly those given in table 3.

Furthermore, the surface scaling dimensions for the DS walk model [20] have been identified

$$x_L^s = L(L-1)/6 \tag{39}$$

where if $x_L^s \leqslant 1$ it is associated with a relevant scaling field. The values of this formula, for $L = 1, 2$ and 3, are precisely those we have found from the MKGW. (This one set of scaling dimensions seems to relate to both the ordinary and special points of the DS model.) A finite-size corrections calculation with appropriate boundary conditions on the Nienhuis O(0) model should demonstrate that this formula also holds for IMSAW.

Finally, we mention that the case with $v \neq w$ with $v + w = 1$ is pertinent to the Ruijgrok–Cohen mirror model [41] with unequal concentrations of left and right scatters $c_{\text{left}} \neq c_{\text{right}}$ with total concentration $c_{\text{left}} + c_{\text{right}} = 1$. This anisotropy is known not to effect the critical indices of the exactly solvable model and hence one need only consider the lattice gas of equal concentrations of scatterers, $c_{\text{left}} = c_{\text{right}} = 1/2$, to study universal features. Note that the unequal concentrations of left and right scatterers does not change the global probability of turning left as opposed to right which is still 1/2 (as any path can be followed in reverse).

Therefore, by this mapping of the seven-vertex Nienhuis model on the square lattice to IMSAW, all the exponents found from MKGW can be confirmed by exact calculation. We note that this system is related to the Coulomb gas [8] with coupling $g = 2/3$.

4. Conclusion

In this paper we have presented techniques for extracting thermal and surface quantities for interacting static-walk problems from KGW simulations. We have stochastically enumerated KGW on the Manhattan lattice, up to lengths of 10^6, which have previously been shown to map to the problem of interacting self-avoiding walks at an inverse temperature of $\beta = (\log 2)/2$. It is also related to the Ruijgrok–Cohen Lorentz lattice gas [42]. This temperature can be seen to be the θ-temperature. Our simulations allow the conjecture of a complete set of relevant exponents and hence scaling dimensions of the static problem. The crossover exponent $\phi = 3/7$ is the same as for the Duplantier and Saleur model [10]. However, it is intriguing to note that the Manhattan walk model contains only nearest-neighbour interactions. Also, a point that warrants attention is that most other numerical estimates of ϕ for collapse problems, including the canonical nearest-neighbour ISAW on a square lattice, rely on information from relatively short walks $N < 300$. Hence, it is interesting to examine the values found from our procedure for Manhattan walks. When the lengths of the simulated KGW are restricted to $N < 300$ the exponent estimates found are still reasonably close to the exact values for all the exponents except the crossover exponent. The crossover exponent can be estimated at a value near 0.50 and almost surely above 0.47,

one would believe, though with a strong drift. We point out that there is also a strong drift in the estimates of the surface-crossover exponent ϕ_s. This may explain recent Monte Carlo results on the interacting self-avoiding walks system [21]. It is also of interest to note that only one of the relevant scaling dimensions differs between the two models. KGW have previously been shown to trace out the hulls of percolation clusters. In percolation the crossover between $(p - p_c)$, the distance to the percolation transition, and the length of the hulls is controlled by the same crossover exponent. This indicates that the identification of the thermal scaling field in the walk problem to the percolation probability in the percolation problem is a valid one.

Another intriguing result of this paper is that, in addition to the established fact that the θ-point of this model is simulated by a kinetic walk (with bulk-interactions given by 'reflection' of the walk from itself), the special point is given by a kinetic walk interacting with a 'reflecting' surface. The critical inverse temperature for surface absorption has been shown to be at $\beta_s = (\log 2)/2$ for the Manhattan lattice θ-point.

All these results are put in context since we have also shown that the static problem of walks on the Manhattan lattice at the θ-temperature can be mapped onto a seven vertex Nienhuis O(n) model with $n = 0$ which in turn is related to the Potts model with $q = 1$. The $q = 1$ Potts model is itself related to percolation. Some of the bulk scaling dimensions have already been calculated via finite-size corrections and concur with our predictions from the kinetic growth model. It would be of interest to verify the surface exponents in a similar way.

Acknowledgments

The authors take pleasure in thanking Murray Batchelor, Richard Brak, Omar Foda, Tony Guttmann, Paul Pearce and Flavio Seno for many fruitful discussions and are grateful to the Australian Research Council for financial support.

References

[1] Flory P 1953 *Principles of Polymer Chemistry* (Ithaca, NY: Cornell University Press)
[2] de Gennes P-G 1979 *Scaling Concepts in Polymer Physics* (Ithaca, NY: Cornell University Press)
[3] des Cloizeaux J and Jannink G 1990 *Polymers in Solution* (Oxford: Clarendon)
[4] de Gennes P-G 1972 *Phys. Lett.* **38A** 339
[5] des Cloizeaux J 1975 *J. Physique* **36** 281
[6] Gujrati P D 1981 *Phys. Rev.* **24** 2096
[7] Cardy J L 1987 *Phase Transitions and Critical Phenomena* vol 11, ed C Domb and J L Lebowitz (New York: Academic)
[8] Nienhuis B 1986 *Phase Transitions and Critical Phenomena* vol 11, ed C Domb and J L Lebowitz (New York: Academic)
[9] Duplantier B 1990 *Phys. Rep.* **184** 229
[10] Duplantier B and Saleur H 1987 *PRL* **59** 539
[11] Poole P H, Coniglio A, Jan N and Stanley H E 1988 *Phys. Rev. Lett.* **60** 1203
[12] Duplantier B and Saleur H 1988 *Phys. Rev. Lett.* **60** 1204
[13] Meirovitch H and Lim H A 1989 *Phys. Rev. Lett.* **62** 2640
[14] Duplantier B and Saleur H 1989 *Phys. Rev. Lett.* **62** 2641
[15] Seno F, Stella A L and Vanderzande C 1988 *Phys. Rev. Lett.* **61** 1520
[16] Duplantier B and Saleur H 1988 *Phys. Rev. Lett.* **61** 1521
[17] Duplantier B and Saleur H 1989 *PRL* **62** 1368
[18] Vanderzande C, Stella A L and Seno F 1991 *Phys. Rev. Lett.* **67** 2757
[19] Chang I and Meirovitch H 1992 *Phys. Rev. Lett.* **69** 2232

[20] *Stella A, Seno F and Vanderzande C 1993 Preprint* Oxford *OUTP-93-03S*
[21] Chang I and Meirovitch H 1993 *Phys. Rev.* E **48** 3656
[22] Seno F and Stella A L 1988 *J. Physique* **49** 739
[23] Meirovitch H and Lim H A 1989 *J. Chem. Phys.* **91** 2544
[24] Maes D and Vanderzande C 1990 *Phys. Rev.* A **41** 3074
[25] Derrida B and Saleur H 1985 *J. Phys. A: Math. Gen.* **18** L1075
[26] Brak R, Owczarek A L and Prellberg T 1993 *J. Phys. A: Math. Gen.* **26** 4565
[27] Coniglio A, Jan N, Majid I and Stanley H E 1987 *Phys. Rev.* B **35** 3617
[28] Majid I, Jan N, Coniglio A and Stanley H E 1984 *Phys. Rev. Lett.* **52** 1257
[29] Lyklema J and Kremer K 1984 *J. Phys. A: Math. Gen.* **17** L691
[30] Kremer K and Lyklema J 1985 *J. Phys. A: Math. Gen.* **18** 1515
[31] Weinrib A and Trugman S A 1985 *Phys. Rev.* B **31** 2993
[32] Ziff R M 1986 *Phys. Rev. Lett.* **56** 545
[33] Saleur H and Duplantier B 1987 *Phys. Rev. Lett.* **58** 2325
[34] Bennett-Wood D, Owczarek A L and Prellberg T 1994 *Physica* A to be published
[35] Bradley R M 1989 *Phys. Rev.* A **39** 3738
[36] Bradley R M 1990 *Phys. Rev.* A **41** 914
[37] Gunn J M F and Ortuno M 1985 *J. Phys. A: Math. Gen.* **18** L1095
[38] Roux S, Guyon E and Sornette D 1985 *J. Phys. A: Math. Gen.* **21** L475
[39] Manna S S and Guttmann A J 1989 *J. Phys. A: Math. Gen.* **22** 3113
[40] Bunimovitch L A and Troubetzkoy S E Recurrence properties of lorentz lattice gas cellular automata *Preprint* University of Bielefeld
[41] Ruijgrok T M and Cohen E G D 1988 *Phys. Lett.* **133** 415
[42] Ziff R M, Kong X P and E G D Cohen 1991 *Phys. Rev.* A **44** 2410
[43] Prellberg T and Seno F in preparation
[44] Nienhuis B 1990 *Int. J. Mod. Phys.* B **4** 929
[45] Blote H W J and Nienhuis B 1989 *J. Phys. A: Math. Gen.* **22** 1415
[46] Batchelor M T 1993 *J. Phys. A: Math. Gen.* **26** 3733
[47] Batchelor M T and Suzuki J 1993 *J. Phys. A: Math. Gen.* **26** L729
[48] Knuth D 1969 *The Art of Computer Programming, Vol. 3: Sorting and Searching* (Reading, MA: Addison Wesley)
[49] L'Ecuyer P and Cote S 1991 *ACM Trans. on Math. Soft.* **17** 98
[50] L'Ecuyer P 1988 *Commun. ACM* **31** 742
[51] Coddington P 1993 *Preprint* Syracuse University *SSCS 526*
[52] Vattubinen I, Kaala K K, Saarinen J and Ala-Nissila T 1993 *Preprint* Tampera University
[53] Grassberger P 1993 *Preprint* Wuppertal WUB 93-03
[54] Stanley H E 1974 *Phase Transitions and Critical Phenomena* vol 3, ed C Domb and M S Green (New York: Academic)
[55] Domany E, Mukamel D, Nienhuis B and Schwimmer A 1981 *Nucl. Phys.* B **190** 279
[56] Baxter R J 1982 *J. Stat. Phys.* **28** 1
[57] Baxter R J 1982 *Exactly Solved Models in Statistical Mechanics* (London: Academic)
[58] Foda O private communication